Finite-Time Sliding Mode Control of Vehicle Formations Considering Performance Constraints

Dongyang Guo, Zhao Zhang, Hongyan Zhou, and Xue-Bo Chen

Abstract—**This article proposes a finite-time control method that integrates sliding mode control with neural networks. The aim is to address the vehicle formation tracking control problem under performance constraints. The core advantage of this method lies in its ability to ensure the stability of the vehicle formation within a finite time. It also meets the specified tracking performance requirements during this process. Specifically, performance functions are first introduced to constrain the tracking performance of each vehicle. Transformation functions are then used to convert the system with these performance constraints into an unconstrained form. This provides a more concise framework for subsequent control design. Next, a sliding surface is designed within the transformed system. This design effectively mitigates the chattering phenomenon commonly observed in traditional sliding mode control. As a result, the robustness and stability of the system are enhanced. To address uncertainties in the system, a neural network approach is employed for system modeling and optimization. The powerful approximation capability of neural networks is utilized to handle nonlinearities and uncertainties in the system. Additionally, a robust term is introduced to counteract potential errors during neural network reconstruction. This further improves the precision and robustness of the control system. Finally, simulation experiments are conducted on the MATLAB platform. The proposed algorithm is compared in detail with existing control methods. The experimental results validate that the proposed algorithm ensures system performance and stability while achieving superior control effectiveness.**

Index Terms—**finite-time; performance constraint; sliding mode control; vehicle formation; neural network**

I. INTRODUCTION

Vehicle formation cooperative control is one of the core technologies of Intelligent Transport Systems, highly valued for its potential to enhance transport efficiency, improve safety and reduce energy loss [1-3]. Vehicle formation cooperative control is used to control multiple vehicles, keeping multiple vehicles traveling at the same distance and speed, improving road operational efficiency and increasing reliability [4, 5].

Nowadays, the main vehicle formation control methods are the pilot-following method [6], artificial potential field method [7], virtual structure method [8], etc. The driver-following method is a method, which controls the entire convoy by controlling the lead vehicle. simplifies the process of designing a controller, have wide-ranging applications.

Currently, research for vehicle models has matured, Common vehicle models are second-order [9] and third-order models [10]. However, due to the complexity of vehicle systems and the diversity of roads travelled, the third-order dynamics model is closer to the actual vehicle. The spacing strategy of vehicle formations directly affects road traffic throughput. Common spacing strategies are constant spacing strategies (CS) [11] and non-linear spacing strategies (NS) [12]. The ideal inter-vehicle distance for CS strategy is a constant, and can increase road availability, but reduces road capacity [13]. Ideal inter-vehicle distance for NS strategy as a non-linear function of vehicle state, Increased road availability and flexibility, NS contains a quadratic spacing strategy and an exponential spacing strategy [14]. Literature [15] proposes a quadratic spacing strategy, balances the stability and capacity of the traffic flow, enhances the stability of the vehicle formations. The current control methods for vehicle formation control are adaptive control [16], consistency control [17], predictive control [18], sliding mode control [19] and so on. During vehicle operation, various uncertainties and external disturbances are often encountered, and sliding mode control is widely used due to its high immunity to disturbances. Literature [20, 21] proposes an integral sliding mode control method, to achieve formation stability. Literature [22] proposes a robust two-way fleet controller, can estimate the mismatch perturbation of adjacent vehicles, however, they are only for second-order systems and are only asymptotically stable.

Finite-time control is widely used because of its advantages such as fast response, high disturbance immunity and high control accuracy. Literature [23, 24] designed finite-time controllers based on third-order models， to solve the fleet problem, but ignored the transient performance of the formation. Literature [25, 26] studies the problem of formation control with specified performance constraints. Literature [27] further investigated finite time formation control with constraints. Literature [28, 29] introduces performance functions, which allow the tracking error to converge to a specified range in finite time, but it does not consider the problem of strong formation stability.

During actual formation control, there are a variety of unknown factors that can affect the system, neural network has strong learning ability and nonlinear approximation

Manuscript received February 27, 2025; revised May 20, 2025. The research work was supported by the Fundamental Research Funds for the Liaoning Universities (LJ212410146025).

Dongyang Guo is a graduate student at the School of Electronic and Information Engineering, University of Science and Technology Liaoning, Anshan, 114051, China. (e-mail: guodongyang1@qq.com).

Zhao Zhang is an associate professor of School of Computer Science and Software Engineering, University of Science and Technology Liaoning, Anshan, 114051, China. (corresponding author, e-mail: zhangzhao333@hotmail.com).

Hongyan Zhou is a doctoral student of School of Electronic and Information Engineering, University of Science and Technology Liaoning, Anshan, 114051, China. (e-mail: zhou321yan@163.com).

Xue-Bo Chen is a professor of School of Electronic and Information Engineering, University of Science and Technology Liaoning, Anshan, 114051, China. (e-mail: xuebochen@126.com).

ability, which can offset the negative impact of these uncertainties on system control, and as such it received a great deal of attention.

Based on the above analysis, the main innovations of this paper are concluded as follows:

(1) This paper uses performance functions to constrain the performance of third-order vehicular systems. This enables the tracking error to converge to the constraint range in finite time, ensuring fast convergence.

(2) To ensure the stability of the system, this paper presents an improved sliding mode control method, eliminates vibration shaking in sliding mode, and incorporates a neural network, using neural networks to approximate complex fuzzy dynamics in control processes, adaptive and robust terms are used to overcome the external interference and the reconstruction error of the neural network.

The overall structure of this paper is as follows: Section 2 presents the system model and control objectives of the vehicle formation of. Section 3 designs the system controller and performs stability analysis. In Section 4, the controller is verified by simulation using real values. Section 5 concludes the paper.

II. Problem Description

A. Vehicle mode

Consider a formation consisting of a leader vehicle and several followers on a straight road, as shown in Fig.1.

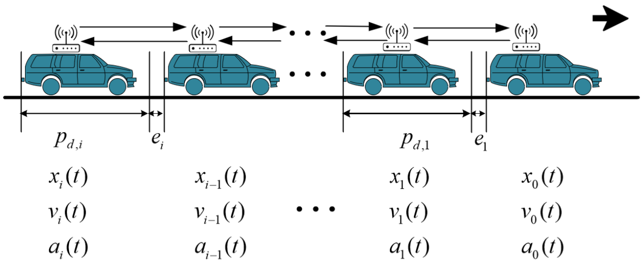

Fig. 1. Vehicle formation model

In the figure, $x_i(t)$, $v_i(t)$, $a_i(t)$ represents the position, velocity and acceleration of the vehicle i respectively. $P_{d,i}$ represents the required spacing between adjacent vehicles. e_i is the error between the actual spacing and the ideal spacing during the driving of the fleet, which is called spacing error.

A single vehicle's third-order kinematics and dynamics model is:

$$\begin{cases} \dot{x}_i(t) = v_i(t), \\ \dot{v}_i(t) = a_i(t) \\ \dot{a}_i(t) = \dfrac{u_i(t)}{m_i\delta} - \dfrac{1}{m_i\delta}[\Gamma(v_i^2 + 2v_i\delta a_i) + F_d] - \dfrac{1}{\delta}a_i(t) + \Delta_i(t) \end{cases} \tag{1}$$

where $u_i(t)$ is the control input, m_i is the actual mass of the vehicle i , δ is the engine time constant in vehicle operation, Γ is the wind resistance of the vehicle during travelling, $\Gamma = \frac{\alpha A_i \varphi}{2}$, α is the density of the air around the vehicle, A_i is the cross-sectional area of the vehicle i subjected to wind resistance, φ is the coefficient of air resistance, F_d is the frictional resistance of the tyres when the vehicle is in motion. Consider road conditions, $F_d = c_i m_i g\cos\theta + m_i g\sin\theta$, c_i is the rolling resistance coefficient of the tyres, θ is the slope of the road surface, $\Delta_i(t)$ is the concentrated disturbance caused by external factors. It is assumed that all vehicles are produced from the same batch and that vehicle dimensions, engine and tyre data remain the same during vehicle formation travel.

B. spacing strategy

This paper gives full consideration to the various aspects of the vehicle in the process of travelling, proposes a quadratic spacing strategy, which sets the ideal inter-vehicle spacing as a quadratic function concerning velocity. The expression is:

$$e_i = x_{i-1} - x_i - d_{1,i} - d_2 - t_s v_i(t) - \frac{\beta v_i^2(t)}{2a_n} \tag{2}$$

where $X_{d,i} = x_{i-1} - x_i$ represents the actual distance between adjacent vehicles. $P_{d,i} = d_{1,i} + d_2 + t_s v_i(t) + \frac{\beta v_i^2(t)}{2a_n}$ represents the desired spacing between adjacent vehicles, the ideal distance includes the length of the vehicle as well as the safety distance required to start and stop the vehicle. $d_{1,i}$ is the length of the i vehicle, d_2 is the safety distance allowed between adjacent vehicles, t_s is the braking time for braking in an emergency, $t_s v_i(t)$ denotes the stopping distance, β represents the safety factor in the external environment, a_n denotes the absolute value of acceleration during acceleration and deceleration..

C. control objective

The requirement of this paper is to design a new finite time control strategy. When the leader vehicle is driving in any state, the following vehicle can quickly track the leader vehicle and achieve performance constraints in a limited time. Specific control objectives are as follows:

(1) Finite-time performance constraints: The fleet is stable and meets the performance constraints in a finite time:

$$-\xi\theta_i(t) \le e_i \le \xi\theta_i(t) \tag{3}$$

$$\begin{cases} \lim\limits_{t \to T} \|e_i\| \le \xi\theta_i(t), \\ v_i(t) \to v_0(t) \\ a_i(t) \to a_0(t) \end{cases} \tag{4}$$

where $\theta_i(t)$ is the performance function， ξ is a constant.

$$\theta_i(t) = (\theta_0 - \theta_\infty)e^{-rt} + \theta_\infty \tag{5}$$

(2) Strong formation stability: the spacing error decreases in steps and does not propagate upstream vehicles along the formation, as described below:

$$|E_i(s)| \le |E_{i-1}(s)| \le \cdots \le |E_1(s)| \tag{6}$$

the error transfer function $G_i(s)=\dfrac{E_{i+1}(s)}{E_i(s)}$ satisfies $\left|G_i(s)\right|\le 1$, where $E_i(s)$ denotes the Laplace transform of $e_i(t)$.

(3) Traffic flow stability: after system stabilization, the derivative of traffic volume D with respect to traffic density ρ is positive.

D. prerequisite knowledge

Lemma 1[30] For a nonlinear system $\dot{x}=f(x,u)$, if there exists a positive definite function $V(x)$ and exist parameters $a,b>0$ and $0<r<1$ such that

$$\dot{V}(x)\le -aV(x)-bV^r(x),t>0 \tag{7}$$

Then the system is exponentially stable and faster finite time stable. The convergence time depends on the initial state $x(0)=x_0$, which is given by

$$T_x(x_0)\le \frac{1}{a(1-r)}\ln\frac{aV^{1-r}(x_0)+b}{b} \tag{8}$$

Lemma 2[15] Equivalence of coupled sliding mode surfaces and each sliding mode surface: at the same time, when and only when s_i is zero, N_i also converges to zero.

$$\mathrm{N}_i(t)=\begin{cases}\mathcal{F}s_i(t)-s_{i+1}(t), & i=1,2,\cdots n-1\\ \mathcal{F}s_i(t), & i=n\end{cases} \tag{9}$$

where $\mathcal{F}$ is the weighting factor and the relationship between N_i and s_i is described as $\mathrm{N}_i(t)=F s_i(t)$, $s=[s_1\ s_2\ \dots\ s_n]$, $N=[N_1\ N_2\ \dots\ N_n]$. F is

$$F=\begin{bmatrix}\mathcal{F} & -1\ \dots\ 0 & 0\\ 0 & \mathcal{F} & -1\ \dots & 0\\ & \vdots & & \\ 0 & 0\ \cdots & \mathcal{F} & -1\\ 0 & 0\ \cdots & 0 & \mathcal{F}\end{bmatrix} \tag{10}$$

Lemma 3[28] For a nonlinear function $f(x):R^n\to R$, there exists an ideal weight vector W and an arbitrarily small positive constant ε enabling the neural network to approximate $f(x)$ in the following way:

$$f(x)=W^T h(X)+\varepsilon \tag{11}$$

where $W\in\mathbb{R}^n$ is the ideal weight matrix of the output layer of the neural network, $\varepsilon\in\mathbb{R}$ is the reconstruction error of the neural network approximation, and $h(X)$ is the activation function.

III. CONTROL METHODS

A. system transformation

The system (1) is a dynamic model of the vehicle, while the control object is the spacing error (2), to make the control objective (3) independent of the system (1), we choose the new state variable as:

$$\begin{cases}y_{1,i}=x_{i-1}-x_i-d_{1,i}-d_2-t_s v_i(t)-\dfrac{\beta {v_i}^2(t)}{2a_n}\\ y_{2,i}=v_{i-1}-v_i-t_s a_i(t)-\dfrac{\beta v_i(t)a_i(t)}{a_n}\end{cases} \tag{12}$$

Deriving it and combining it with the dynamics model of the vehicle (1), we can obtain the new system:

$$\begin{cases}\dot{y}_{1,i}=y_{2,i}\\ \dot{y}_{2,i}=[\dfrac{u_i(t)}{m_i\delta}+\Delta_i(t)+f(v_i,a_i)][-t_s-\dfrac{\beta v_i(t)}{a_n}]\end{cases} \tag{13}$$

where

$$f(v_i,a_i)=-\frac{1}{m_i\delta}[\Gamma({v_i}^2+2v_i\delta a_i)+F_d]-\frac{1}{\delta}a_i(t)-\frac{a_{i-1}-a_i-\dfrac{\beta a_i^2(t)}{a_n}}{t_s+\dfrac{\beta v_i(t)}{a_n}} \tag{14}$$

The performance constraint is (3), to facilitate the calculation, transform the objective constraints so that constrained become unconstrained:

$$y_{1,i}\in(-\xi\Theta_i(t),\xi\Theta_i(t))\to Z(y_{1,i})\in(-\infty,+\infty) \tag{15}$$

that is:

$$\begin{cases}\lim_{y_{1,i}\to\ \xi\Theta_i(t)} Z(y_{1,i})=+\infty\\ \lim_{y_{1,i}\to -\xi\Theta_i(t)} Z(y_{1,i})=-\infty\end{cases} \tag{16}$$

where $Z(y_{1,i})$ is a function for $y_{1,i}$, when $Z(y_{1,i})\in(-\infty,+\infty)$, get $y_{1,i}\in(-\xi\Theta_i(t),\xi\Theta_i(t))$, as long as $Z(y_{1,i})$ is bounded, the performance constraints of $y_{1,i}$ can be satisfied.

The transformation function $Z(y_{1,i})$ is calculated as:

$$Z(y_{1,i})=\frac{1}{2}\ln(\frac{y_{1,i}+\xi\Theta_i(t)}{\xi\Theta_i(t)-y_{1,i}}) \tag{17}$$

For convenience, $z_{1,i}$ is used instead of $Z(y_{1,i})$, and the second-order derivative of $z_{1,i}$ is obtained:

$$\begin{cases}\dot{z}_{1,i}=\dfrac{\partial Z(y_{1,i})}{\partial y_{1,i}}+\dfrac{\partial Z(y_{1,i})}{\partial\xi\Theta_i(t)}\\ \ddot{z}_{1,i}=\dfrac{\partial^2 Z(y_{1,i})}{\partial {y_{1,i}}^2}+\dfrac{\partial^2 Z(y_{1,i})}{\partial y_{1,i}\partial\xi\Theta_i(t)}+\dfrac{\partial^2 Z(y_{1,i})}{\partial\xi\Theta_i(t)\partial y_{1,i}}+\dfrac{\partial^2 Z(y_{1,i})}{\partial\xi\Theta_i(t)^2}\end{cases} \tag{18}$$

where

$$\begin{cases}\dfrac{\partial^2 Z(y_{1,i})}{\partial {y_{1,i}}^2}=\dfrac{2y_{1,i}{y_{2,i}}^2\xi\Theta_i}{[(\xi\Theta_i)^2-{y_{1,i}}^2]^2}+\dfrac{\xi\Theta_i\,\dot{y}_{2,i}}{(\xi\Theta_i)^2-{y_{1,i}}^2}\\ \dfrac{\partial^2 Z(y_{1,i})}{\partial y_{1,i}\partial\xi\Theta_i(t)}=\dfrac{-{y_{1,i}}^2y_{2,i}\xi\dot{\Theta}_i-y_{2,i}\xi\dot{\Theta}_i(\xi\Theta_i)^2}{[(\xi\Theta_i)^2-{y_{1,i}}^2]^2}\\ \dfrac{\partial^2 Z(y_{1,i})}{\partial\xi\Theta_i(t)\partial y_{1,i}}=\dfrac{-{y_{1,i}}^2y_{2,i}\xi\dot{\Theta}_i-y_{2,i}\xi\dot{\Theta}_i(\xi\Theta_i)^2}{[(\xi\Theta_i)^2-{y_{1,i}}^2]^2}\\ \dfrac{\partial^2 Z(y_{1,i})}{\partial\xi\Theta_i(t)^2}=\dfrac{-y_{1,i}(\xi\Theta_i)^2\xi\ddot{\Theta}_i+{y_{1,i}}^3\xi\ddot{\Theta}_i+2y_{1,i}\xi\Theta_i(\xi\dot{\Theta}_i)^2}{[(\xi\Theta_i)^2-{y_{1,i}}^2]^2}\end{cases} \tag{19}$$

We can get the new system:

$$\begin{cases} \dot{z}_{1,i} = z_{2,i} \\ \dot{z}_{2,i} = \dfrac{\partial^2 Z(y_{1,i})}{\partial y_{1,i}\partial \xi\Theta_i(t)} + \dfrac{\partial^2 Z(y_{1,i})}{\partial \xi\Theta_i(t)\partial y_{1,i}} + \dfrac{\partial^2 Z(y_{1,i})}{\partial \xi\Theta_i(t)^2} + \dfrac{2y_{1,i}y_{2,i}{}^2\xi\Theta_i}{[(\xi\Theta_i)^2 - y_{1,i}{}^2]^2} + \\ \qquad \dfrac{\xi\Theta_i}{(\xi\Theta_i)^2 - y_{1,i}{}^2}[\dfrac{u_i(t)}{m_i\delta} + \Delta_i(t) + f(v_i, a_i)][-t_s - \dfrac{\beta v_i(t)}{a_n}] \end{cases} \tag{20}$$

It can be controlled by controlling the new system (20), thus achieving our control goals.

B. slide mode control

Based on the converted system (20), an improved sliding mode surface is designed:

$$s_i = z_{2,i} + \lambda\chi(z_{1,i}) \tag{21}$$

where the $\chi(z_{1,i})$ function is

$$\chi(z_{1,i}) = \begin{cases} |z_{1,i}|^\gamma \operatorname{sgn}(z_{1,i}) & s = 0 \ or \ s \neq 0, |z_{1,i}| > \upsilon \\ l_1 z_{1,i} + l_2 |z_{1,i}|^2 \operatorname{sgn}(z_{1,i}) & s \neq 0, |y_{1,i}| < \upsilon \end{cases} \tag{22}$$

where $\frac{1}{2} < \gamma < 1$, γ is a fraction where both the numerator and denominator are positive odd numbers, $\upsilon > 0$ is a positive number with a small value, $l_1 = (2-\gamma)\upsilon^{\gamma-1}$, $l_2 = (\gamma-1)\upsilon^{\gamma-2}$.

When $s_i = 0$, $z_{2,i} = -\lambda\chi(z_{1,i})$, that is

$$z_{2,i} = \begin{cases} -\lambda|z_{1,i}|^\gamma \operatorname{sgn}(z_{1,i}) & s = 0 \ or \ s \neq 0, |z_{1,i}| > \upsilon \\ -\lambda l_1 z_{1,i} - \lambda l_2 |z_{1,i}|^2 \operatorname{sgn}(z_{1,i}) & s \neq 0, |z_{1,i}| < \upsilon \end{cases} \tag{23}$$

when $|z_{1,i}| < \upsilon$, $z_{2,i} = -\lambda l_1 z_{1,i} - \lambda l_2 |z_{1,i}|^2 \operatorname{sgn}(z_{1,i})$ converges faster than $z_{2,i} = -\lambda|z_{1,i}|^\gamma \operatorname{sgn}(z_{1,i})$, this indicates that the improved new sliding mode surface has a faster convergence rate..

The traditional sliding mode control is affected by various factors, which will lead to chattering on the sliding mode surface. Therefore we use the saturation function (24) instead of instead of the sign function, where η is a small positive number representing the thickness of the sliding mode boundary layer.

$$sat(s) = \begin{cases} 1 & s > \eta \\ ks, k = \dfrac{1}{\eta} & |s| \leq \eta \\ -1 & s < -\eta \end{cases} \tag{24}$$

Derivative with respect to the sliding mode:

$$\dot{s}_i = \dot{z}_{2,i} + \lambda\dot{\chi}(z_{1,i}) \tag{25}$$

Introducing a coupled slide mould surface

$$\mathrm{N}_i(t) = \begin{cases} \mathcal{C}s_i(t) - s_{i+1}(t), i = 1, 2, \cdots n-1 \\ \mathcal{C}s_i(t), i = n \end{cases} \tag{26}$$

where $\mathcal{C}$ satisfies $0 < \mathcal{C} \leq 1$.

Recalling(26) shows that $\mathrm{N}_i(t)$ and $s_i(t)$ have the same convergence.

The derivative of $\mathrm{N}_i(t)$ is as follows:

$$\dot{\mathrm{N}}_i(t) = \begin{cases} \mathcal{C}[\dot{z}_{2,i} + \lambda\dot{\chi}(z_{1,i})] - \dot{s}_{i+1}, i = 1, 2, \cdots n-1 \\ \mathcal{C}[\dot{z}_{2,i} + \lambda\dot{\chi}(z_{1,i})], i = n \end{cases} \tag{27}$$

C. neural network approximation

Because there is some uncertainty in the system (20), both $y_{1,i}$ and $y_{2,i}$ are computable, we use the RBF neural network to approximate.

$$\begin{aligned} G_i(Y) = {} & M_i(y)\left(\frac{\xi\Theta_i}{(\xi\Theta_i)^2 - y_{1,i}{}^2}[t_s + \frac{\beta v_i(t)}{a_n}]\right)^{-1} - f(v_i, a_i) - \\ & \lambda\dot{\chi}(z_{1,i})\left(\frac{\xi\Theta_i}{(\xi\Theta_i)^2 - y_{1,i}{}^2}[t_s + \frac{\beta v_i(t)}{a_n}]\right)^{-1} - \\ & \dot{s}_{i+1}\left(\mathcal{C}\frac{\xi\Theta_i}{(\xi\Theta_i)^2 - y_{1,i}{}^2}[t_s + \frac{\beta v_i(t)}{a_n}]\right)^{-1} \end{aligned} \tag{28}$$

where

$$M_i(y) = \frac{\partial^2 Z(y_{1,i})}{\partial y_{1,i}\partial \xi\Theta_i(t)} + \frac{\partial^2 Z(y_{1,i})}{\partial \xi\Theta_i(t)\partial y_{1,i}} + \frac{\partial^2 Z(y_{1,i})}{\partial \xi\Theta_i(t)^2} + \frac{2y_{1,i}y_{2,i}{}^2\xi\Theta_i}{[(\xi\Theta_i)^2 - y_{1,i}{}^2]^2} \tag{29}$$

According to Lemma 3, when a neural network approximates an unknown nonlinear function, the neural network $G(Y)$ can be expressed as:

$$G_i(Y) = W_i^T h(Y_i) + \varepsilon \tag{30}$$

where $Y_i = [y_{1,i}, y_{2,i}]$ is the input of the neural network, $W \in \mathbb{R}^n$ is the ideal weights of the output layer of the neural network, $\varepsilon \in \mathbb{R}^n$ is the reconstruction error of the neural network, the activation function is chosen to be a Gaussian function $h(Y) = e^{(\frac{\|Y_i - c_i\|^2}{2b_i^2})}$, where $i = 1, \ldots, m$, m is the number of nodes in the hidden layer, c_i and b_i are constants, $h(\bullet) < \bar{h}$, $\bar{h}$ is a positive number.

Assumption 1. assume that W and the reconstruction error ε are bounded, satisfied $\|W\| \leq w_m$, $\varepsilon \leq \varepsilon_m$. We use $\widehat{W}$ as an estimate of the ideal weights W, defined $\widetilde{W} = W - \widehat{W}$ as the neural network weight estimation error.

D. finite-time controller design

The controller of the system(20) is designed as follows:

$$\begin{aligned} u_i = m_i\delta[& \frac{k_n N_i + k_m \operatorname{sgn}(N_i)}{\mathcal{C}[t_s + \dfrac{\beta v_i(t)}{a_n}]\dfrac{\xi\Theta_i}{(\xi\Theta_i)^2 - y_{1,i}{}^2}} - \Delta_i(t) + k_p \operatorname{sgn}(N_i) \\ & + \widehat{W}^T h(Y_i) + \sigma \operatorname{sgn}(N_i)] \end{aligned} \tag{31}$$

where k_m, k_n, k_p are all positive, $\sigma_i > 0$ is the adaptive variable, used $\widehat{\sigma_i}$ as the estimation of σ_i, defined $\widetilde{\sigma_i} = \sigma_i - \widehat{\sigma_i}$ as the estimation error of the adaptive variable. This paper proposes a robust term $k_p \operatorname{sgn}(N_i)$ to counteract the reconstruction error.

The weight adaptation law $\widehat{W}$ of the neural network in the control process is

$$\dot{\widehat{W}}_i = \tau N_i \mathcal{C}[t_s + \frac{\beta v_i(t)}{a_n}]\frac{\xi\Theta_i}{(\xi\Theta_i)^2 - y_{1,i}{}^2}h(Y) \tag{32}$$

The adaptive law $\hat{\sigma}$ in the control process is

$$\dot{\hat{\sigma}}_i = -\tau N_i \mathcal{C}[t_s + \frac{\beta v_i(t)}{a_n}]\frac{\xi\Theta_i}{(\xi\Theta_i)^2 - y_{1,i}{}^2} \tag{33}$$

In order to prove that the designed control algorithm can meet the control requirements of the whole system, we analyze and verify the control algorithm by using Lyapunov theory. The stability analysis is performed first, followed by finite time analysis, and the following theorem proves the stability of the proposed control algorithm.

Theorem 1. For the vehicle dynamics model (1), combined with the quadratic spacing strategy (2), the control algorithm (31) is designed using the transformed system (20), Combining adaptive laws (32) and (33). The control objectives of this paper can be achieved.

Proof: choose the Lyapunov function.

$$V_i = \frac{1}{2}N_i{}^2 + \frac{1}{2\tau}\widetilde{W}_i{}^T\widetilde{W}_i + \frac{1}{2\tau}\tilde{\sigma}^2 \tag{34}$$

Derivation of (34) yields

$$\dot{V}_i = N_i\dot{N}_i + \frac{1}{\tau}\widetilde{W}_i{}^T\dot{\widetilde{W}}_i + \frac{1}{\tau}\tilde{\sigma}\dot{\tilde{\sigma}} \tag{35}$$

where

$$\begin{aligned} N_i\dot{N}_i &= N_i\left(\mathcal{C}[\dot{z}_{2,i} + \lambda\chi(\dot{z}_{1,i})] - \dot{s}_{i+1}\right) \\ &= N_i\Bigg\{\mathcal{C}\Bigg(\frac{\partial^2 Z(y_{1,i})}{\partial y_{1,i}\partial\xi\Theta_i(t)} + \frac{\partial^2 Z(y_{1,i})}{\partial\xi\Theta_i(t)\partial y_{1,i}} + \frac{\partial^2 Z(y_{1,i})}{\partial\xi\Theta_i(t)^2} + \\ &\quad \frac{2y_{1,i}y_{2,i}{}^2\xi\Theta_i}{[(\xi\Theta_i)^2 - y_{1,i}{}^2]^2} + \frac{\xi\Theta_i}{(\xi\Theta_i)^2 - y_{1,i}{}^2}[\frac{u_i(t)}{m_i\delta} + \Delta_i(t) + \\ &\quad f(v_i, a_i)][-t_s - \frac{\beta v_i(t)}{a_n}] + \lambda\chi(\dot{z}_{1,i})\Bigg) - \dot{s}_{i+1}\Bigg\} \end{aligned} \tag{36}$$

Combining (28), (29) and (30) is obtained using neural network approximation:

$$G_i(Y) = (\widetilde{W} + \widehat{W})h(Y) + \varepsilon \tag{37}$$

Substituting (37) into (36) yields:

$$\begin{aligned} N_i\dot{N}_i = N_i\Bigg\{&\mathcal{C}\frac{\xi\Theta_i}{(\xi\Theta_i)^2 - y_{1,i}{}^2}[t_s + \frac{\beta v_i(t)}{a_n}]\left(\widetilde{W}h(X) + \widehat{W}h(X) + \right. \\ &\left.\varepsilon - \frac{u_i(t)}{m_i\delta} - \Delta_i(t)\right)\Bigg\} \end{aligned} \tag{38}$$

therefore

$$\begin{aligned} \dot{V}_i = N_i\Bigg\{&\mathcal{C}\frac{\xi\Theta_i}{(\xi\Theta_i)^2 - y_{1,i}{}^2}[t_s + \frac{\beta v_i(t)}{a_n}]\left(\widetilde{W}h(X) + \widehat{W}h(X) + \right. \\ &\left.\varepsilon - \frac{u_i(t)}{m_i\delta} - \Delta_i(t)\right)\Bigg\} + \frac{1}{\tau}\widetilde{W}_i{}^T\dot{\widetilde{W}}_i + \frac{1}{\tau}\tilde{\sigma}\dot{\tilde{\sigma}} \end{aligned} \tag{39}$$

Substituting the controller (31) and the adaptive laws (32) and (33) into (39) yields:

$$\begin{aligned} \dot{V}_i = N_i\Bigg\{&\mathcal{C}\frac{\xi\Theta_i}{(\xi\Theta_i)^2 - y_{1,i}{}^2}[t_s + \frac{\beta v_i(t)}{a_n}]\left(\widetilde{W}^T h(X) + \varepsilon - \frac{k_p\,\mathrm{sgn}(N_i)}{\partial}\right. \\ &\left. - \frac{\sigma\,\mathrm{sgn}(N_i)}{\partial}\right)\Bigg\} - k_n N_i - \tilde{\sigma}N_i[t_s + \frac{\beta v_i(t)}{a_n}]\frac{\xi\Theta_i}{(\xi\Theta_i)^2 - y_{1,i}{}^2} \\ &- k_m\,\mathrm{sgn}(N_i) + \widetilde{W}_i{}^T N_i[t_s + \frac{\beta v_i(t)}{a_n}]\frac{\xi\Theta_i}{(\xi\Theta_i)^2 - y_{1,i}{}^2}h(Y) \end{aligned} \tag{40}$$

Simplification of (40) yields:

$$\begin{aligned} \dot{V}_i = &-k_n N_i{}^2 - k_m N_i\,\mathrm{sgn}(N_i) + N_i\mathcal{C}\frac{\xi\Theta_i}{(\xi\Theta_i)^2 - y_{1,i}{}^2}[t_s + \frac{\beta v_i(t)}{a_n}](\varepsilon - \\ &k_p\,\mathrm{sgn}(N_i) - \hat{\sigma}\,\mathrm{sgn}(N_i)) \end{aligned} \tag{41}$$

where $k_p\,\mathrm{sgn}(s)$ is a robust term to counteract the reconstruction error of the neural network approximation, thus

$$\begin{aligned} \dot{V}_i &\le -k_n N_i{}^2 - k_m N_i\,\mathrm{sgn}(N_i) \\ &\le -k_n N_i{}^2 - k_m\left|N_i\right| \end{aligned} \tag{42}$$

Thus, it can be shown that the system is uniformly eventually bounded, and we can know $\left|\widetilde{W}^T h(X)\right| \le \psi$, ψ as a small constant. Next, prove finite time stabilization. Let the Lyapunov function be

$$V_s = \frac{1}{2}N_i{}^2 \tag{43}$$

Deriving it and combining it with neural network yields:

$$\begin{aligned} \dot{V}_i &= N_i\dot{N}_i \\ &= N_i\Bigg\{\mathcal{C}\frac{\xi\Theta_i}{(\xi\Theta_i)^2 - y_{1,i}{}^2}[t_s + \frac{\beta v_i(t)}{a_n}]\left(\widetilde{W}h(X) + \widehat{W}h(X) + \right. \\ &\quad\left.\varepsilon - \Delta_i(t) - \frac{u_i(t)}{m_i\delta}\right)\Bigg\} \end{aligned} \tag{44}$$

Substituting (31) yields:

$$\begin{aligned} \dot{V}_i = &-k_n N_i{}^2 - k_m N_i\,\mathrm{sgn}(N_i) + N_i\mathcal{C}\frac{\xi\Theta_i}{(\xi\Theta_i)^2 - y_{1,i}{}^2}[t_s + \\ &\frac{\beta v_i(t)}{a_n}]\left(\widetilde{W}h(Y) + \varepsilon - k_p\,\mathrm{sgn}(N_i) - \sigma\,\mathrm{sgn}(N_i)\right) \\ \le &-k_n N_i{}^2 + N_i\mathcal{C}\frac{\xi\Theta_i}{(\xi\Theta_i)^2 - y_{1,i}{}^2}[t_s + \frac{\beta v_i(t)}{a_n}]\left(\widetilde{W}h(Y) - \sigma\,\mathrm{sgn}(N_i)\right) \end{aligned} \tag{45}$$

Recall the equation (17) shows that there exists a positive number $\phi > 0$ satisfy $\frac{\xi\Theta_i}{(\xi\Theta_i)^2 - y_{1,i}{}^2} > \phi > 0$, and there exists a small positive number $\&$ satisfy $t_s + \frac{\beta v_i(t)}{a_n} > \& > 0$, it is known that $\sigma > \psi$, assuming that $\pi = \sigma - \psi > 0$, thus

$$\dot{V}_s \le -k_n N_i{}^2 - \mathcal{C}\phi\,\&\,\pi\left|N_i\right| \le -2k_n V_s - \mathcal{C}\phi\,\&\,\pi V_s^{\frac{1}{2}} \tag{46}$$

where $a = 2k_n$, $b = \partial\phi\,\&\,\pi$, it can be shown that the system can reach stability in finite time and it can be shown that $y_{1,i}$ is bounded, so we obtain $y_{1,i} \in (-\xi\theta_i(t), \xi\theta_i(t))$, which satisfies the control objective of the system.

With the above proof it is possible to obtain that $N_i(t)$ converges to a small neighbourhood near zero in finite time, which can be obtained according to (26):

$$\mathcal{C}s_i(t) \approx s_{i+1}(t) \tag{47}$$

because of $0 < \mathcal{C} \le 1$, we can get $0 < \frac{s_{i+1}(t)}{s_i(t)} \le 1$.

The sign-preserving theorem of the limit yields that the transformed pitch tracking error $z_{1,i}$ and the sliding mode surface $s_i(t)$ have the same convergence and the same sign. And because $s_i(t)s_{i+1}(t) \ge 0$, so $z_{1,i}z_{1,i+1} \ge 0$, because $0 < \frac{s_{i+1}(t)}{s_i(t)} \le 1$, so $0 < \frac{z_{1,i+1}}{z_{1,i}} \le 1$, because the converted spacing tracking error $z_{1,i}$ and e_i have the same convergence, so $0 < \frac{\int_0^t e_{i+1}e^{-st}dt}{\int_0^t e_ie^{-st}dt} \le 1$, $0 < \frac{E_{i+1}(s)}{E_i(s)} \le 1$, satisfies strong formation stability.

E. traffic flow stability

$$\rho = \frac{N}{P} = \frac{D}{\overline{V_S}} \tag{48}$$

Where ρ is the traffic density, N is the number of vehicles in the road section, P is the length of the road section, D is the amount of traffic on the lane (flow rate), $\overline{V_S}$ is the average speed of vehicles in the interval. Assuming that the formation system arrives at a steady state, the safety distance of vehicles and the average speed arrives at the same, take the length of the road section P as $P = d_{1,i} + d_2 + t_sv + \frac{\beta v^2}{2a_n}$, the vehicles within the road section N as 1, the average speed $\overline{V_S}$ as v, traffic density as:

$$\rho = \frac{N}{P} = \frac{1}{d_{1,i} + d_2 + t_sv + \frac{\beta v^2}{2a_n}} \tag{49}$$

Then

$$v = \sqrt{(\frac{1}{\rho} - d_{1,i} - d_2)\frac{2a_n}{\beta} + (\frac{t_sa_n}{\beta})^2} - \frac{t_sa_n}{\beta} \tag{50}$$

Derivation of $D = \rho v$:

$$\dot{D} = \sqrt{(\frac{1}{\rho} - d_{1,i} - d_2)\frac{2a_n}{\beta} + (\frac{t_sa_n}{\beta})^2} - \frac{t_sa_n}{\beta} - \frac{a_n}{\rho\beta\sqrt{(\frac{1}{\rho} - d_{1,i} - d_2)\frac{2a_n}{\beta} + (\frac{t_sa_n}{\beta})^2}} \tag{51}$$

From (51) it can be found that when the critical density

$$\rho_s = \frac{1}{2(d_{1,i} + d_2) + t_s\sqrt{\frac{2(d_{1,i} + d_2)a_n}{\beta}}}$$

the derivative $\dot{D}$ is 0, and $\rho > \rho_s$, so $\dot{D} > 0$, the formation achieves traffic flow stability.

IV. SIMULATION EXPERIMENT

To verify the effectiveness of the proposed control algorithm, the vehicle formation is simulated in a MATLAB environment. During the simulation, the convoy consists of a leader vehicle and four follower vehicles travelling in a straight lane. Let the initial state of the leader vehicle be: $x_0(0) = 0$, $v_0(0) = 0$. The initial state of the four following vehicles is $x_i(0) = [-24; -48; -72; -96]$, $v_i(0) = [0;0;0;0]$, $a_i(0) = [0;0;0;0]$。

The time of the simulation experiment is set to $80\,s$, considering the actual situation of the vehicle information, using the same batch of production of the same vehicle, assuming that the parameters of each vehicle are the same, where the parameters of the vehicle are set as follows: mass of the vehicle m_i =1600 kg, air resistance Γ =0.414, running resistance of the vehicle F_d =240, length of the vehicle $d_{1,i}$ =4 m, ideal safe distance d_2 =7 m, safety factor of the external environment of the vehicle β =0.2, braking or acceleration reaction time t_s =0.12 S, maximum deceleration possible value of a_n =7, concentrated disturbance $\Delta_i(t) = 0.1\cos(t)$. In selecting the parameters, with due consideration of the control method and the control objectives, the parameters of the controller are shown in Table I.

TABLE I
CONTROLLER PARAMETERS

ξ	r	γ	υ
0.05	0.8	7 / 9	0.1
λ	k_n	k_m	k_p
0.03	0.03	1	10

The acceleration of the leader vehicle is set to

$$a_0 = \begin{cases} 0.5t\ m/s^2 & 0 \le t < 4s \\ 2t\ m/s^2 & 4 \le t < 8s \\ -0.5t + 6\ m/s^2 & 8 \le t \le 12s \\ 0\ m/s^2 & t > 12 \end{cases}$$

The acceleration of the leader vehicle increases and then decreases, with a steady rate of 16 m/s after 12 S.

A. simulation results

The simulation results of the control algorithm designed in this paper are shown in Fig.2-8. Fig.2 shows the displacement of the formation vehicle, which can be visualized that the displacement of the following vehicle first converges and then always follows the leader vehicle. Fig.3-4 shows the relationship between the speed and acceleration of the vehicles in the formation, and the speed and acceleration can keep the same with the leader vehicle after stabilization. Fig.5 reflects the workshop distance of the formation, the initial value is 24 m, and then it is adjusted with the speed of the vehicles, and finally it is kept at about 14 m, which achieves the ideal workshop distance. Fig.6-7 reflects the slip mode surface and the coupled slip mode surface information, and the slip mode surface converges to zero. Fig. 8 reflects the spacing error information of the formation, and the initial spacing error is 13 m, after which it converges rapidly. The analysis shows that the RBF neural network has good real-time performance, and the formation system can satisfy the performance constraints within 2 S. After that, the formation system continues to converge, and the spacing error can converge to zero in about 4 S, so that the spacing between the vehicles can maintain the ideal state, and thus the stability of the whole fleet of vehicles can be realized.

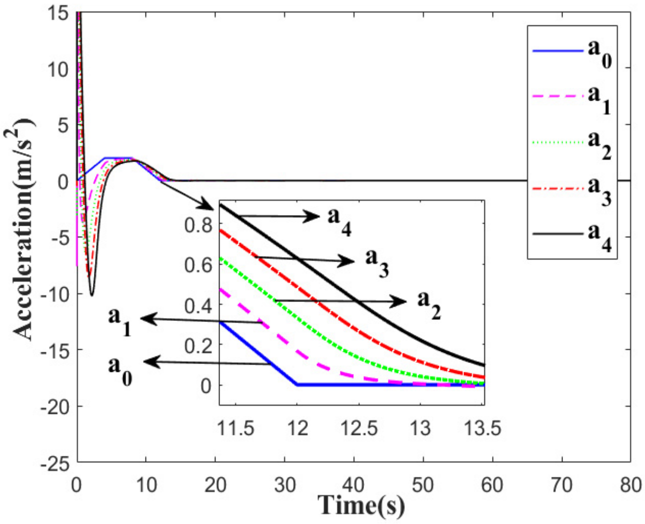

Fig.4. Acceleration of formation vehicles

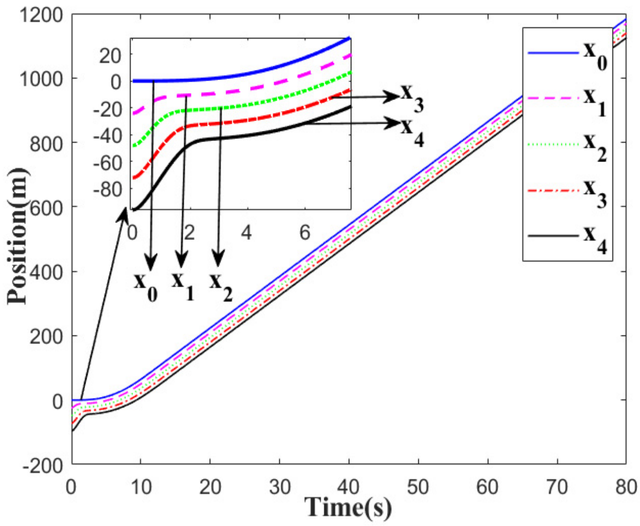

Fig. 2. Displacement of formation vehicles

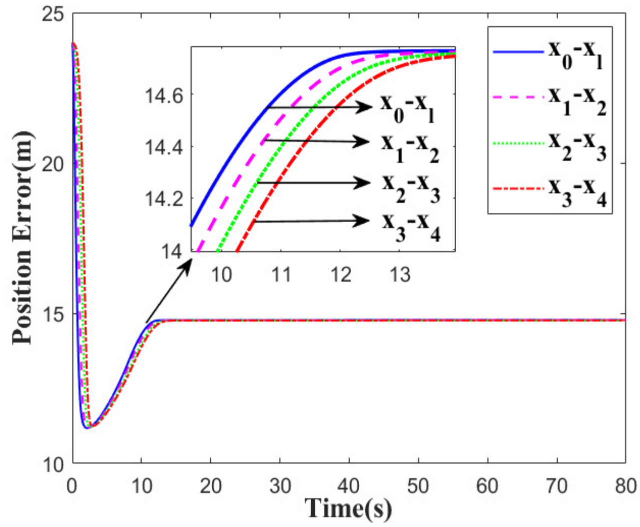

Fig.5. Displacement error of formation vehicles

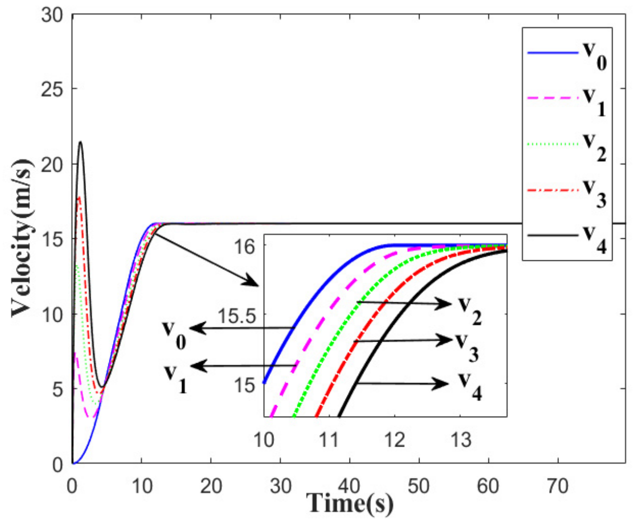

Fig.3. Speed of formation vehicles

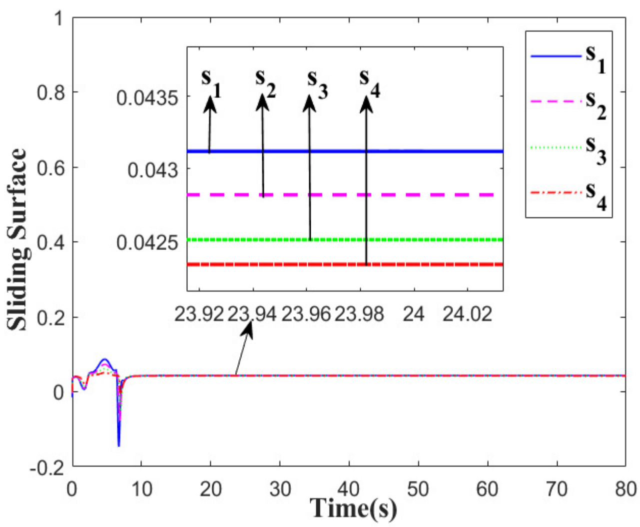

Fig.6. Surface of sliding mode

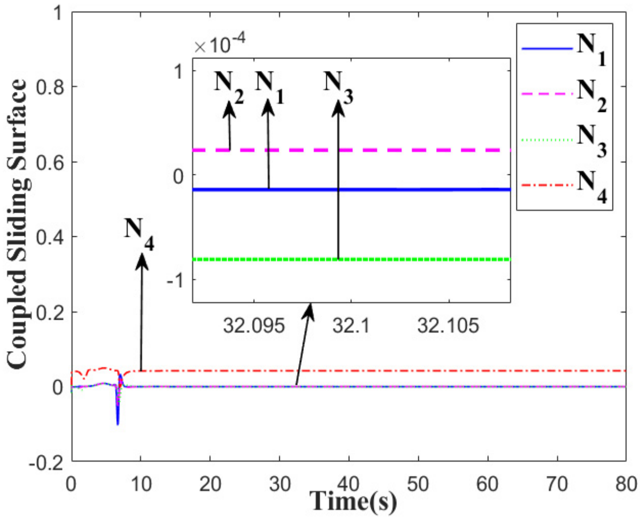

Fig.7. Coupled surface of sliding mode

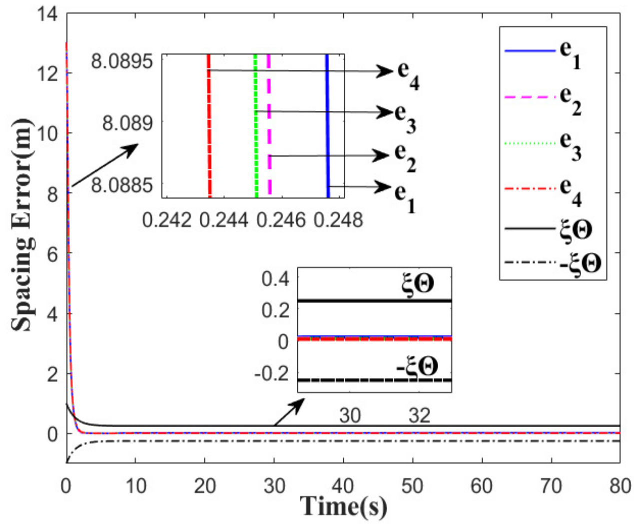

Fig.8. Spacing error of formation vehicles

B. comparative experiment

To further illustrate the performance advantages of the novel control algorithm in this paper, it's compared with the traditional unconstrained control algorithm in literature[31]. Setting the sliding mode function as $s_i = e_i(t) + c\,sign(e_i(t))\left|e_i(t)\right|^{\frac{1}{2}}$. The simulation environment and parameters are consistent with thesis, and the simulation results are shown in Figs.9-15, Fig.9 shows the displacement of the formation vehicle, Fig.10 shows the velocity of the formation vehicle, Fig.11 shows the acceleration of the formation vehicle, and Fig.12 reflects the displacement error of the formation. Fig.13 shows the formation vehicle spacing error, and Fig.14-15 show the slip mode surface and coupled slip mode surface information. The analysis shows that the spacing error converges to 0 around 14. Comparing Figs. 2-8, it can be obtained that the control algorithm proposed in this paper converges about 10 seconds faster than the traditional sliding mode control, and the algorithm in this thesis has a better real-time performance, which is able to better realize the formation control requirements.

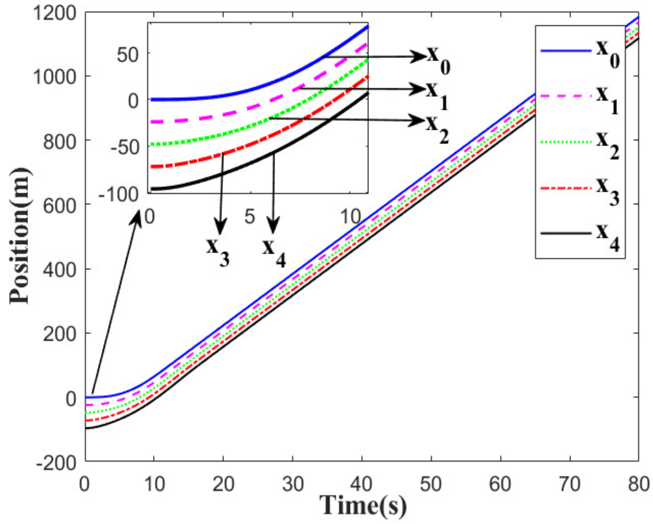

Fig.9. Displacement of formation vehicles

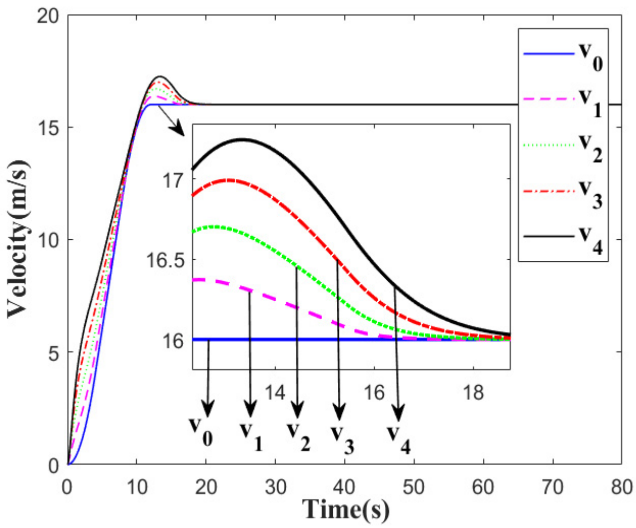

Fig.10. Speed of formation vehicles

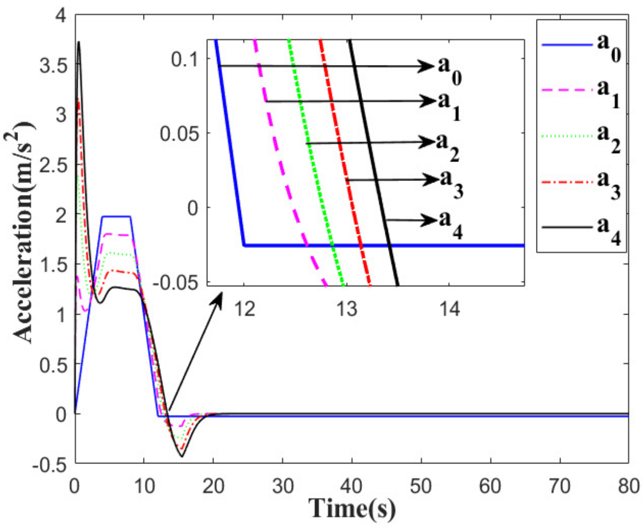

Fig.11. Acceleration of formation vehicles

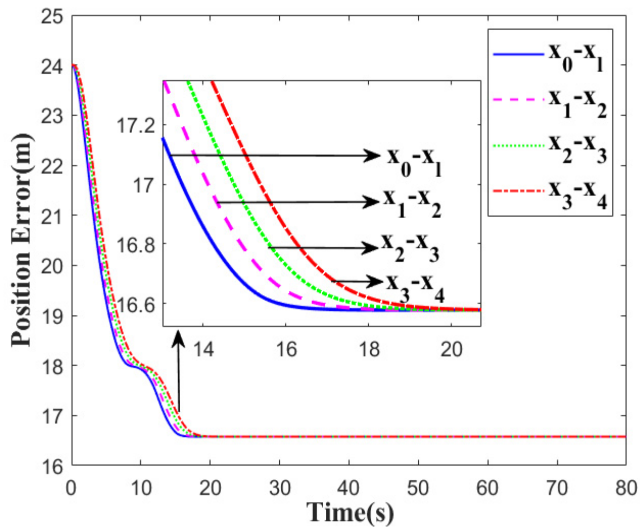

Fig.12. Displacement error of formation vehicles

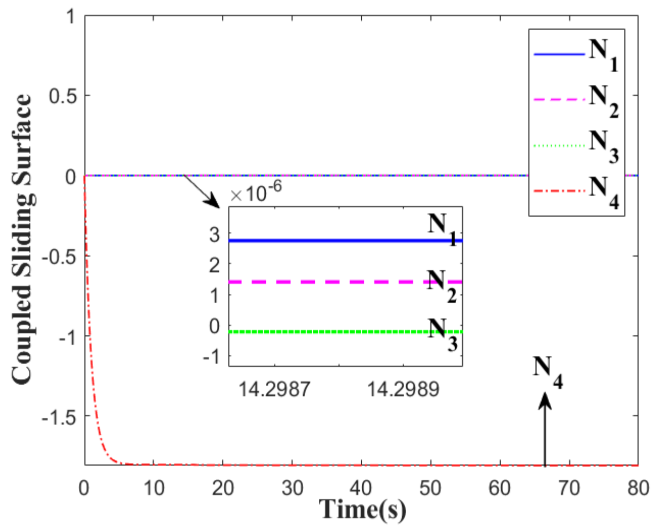

Fig.15. Coupled surface of sliding mode

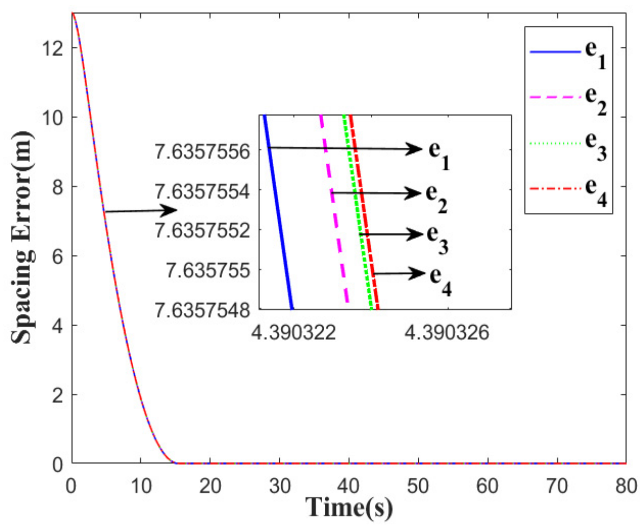

Fig.13. Spacing error of formation vehicles

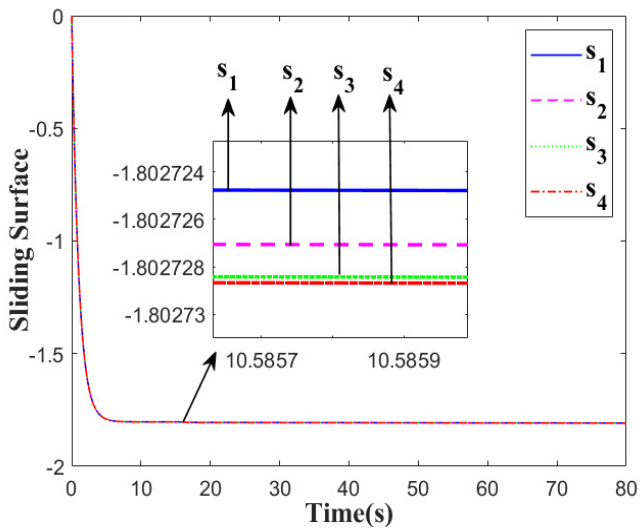

Fig.14. Surface of sliding mode

V. Conclusion

This paper investigates the vehicle queue control problem with performance constraints, performance constraints are implemented using performance functions, so that the tracking error converges to the bounded range in finite time, and applying neural networks to sliding mode control, using neural networks to overcome parameter uncertainty in control processes, ensure the fleet's strong formation stability. In urban road traffic, the horizontal relationship during vehicle traveling is also not to be ignored. In the future, it is of great significance to study the lateral structure of vehicles.

References

[1] S. Chu, and A. Majumdar, "Opportunities and challenges for a sustainable energy future," *Nature,* vol. 488, no. 7411, pp. 294-303, 2012/08/01, 2012.

[2] J. Ding, L. Li, H. Peng *et al.*, "A Rule-Based Cooperative Merging Strategy for Connected and Automated Vehicles," *IEEE Transactions on Intelligent Transportation Systems,* vol. 21, no. 8, pp. 3436-3446, 2020.

[3] X. Ge, Q. L. Han, J. Wang *et al.*, "Scalable and Resilient Platooning Control of Cooperative Automated Vehicles," *IEEE Transactions on Vehicular Technology,* vol. 71, no. 4, pp. 3595-3608, 2022.

[4] J. Hu, P. Bhowmick, F. Arvin *et al.*, "Cooperative Control of Heterogeneous Connected Vehicle Platoons: An Adaptive Leader-Following Approach," *IEEE Robotics and Automation Letters,* vol. 5, no. 2, pp. 977-984, 2020.

[5] Z. Wang, Y. Bian, S. E. Shladover *et al.*, "A Survey on Cooperative Longitudinal Motion Control of Multiple Connected and Automated Vehicles," *IEEE Intelligent Transportation Systems Magazine,* vol. 12, no. 1, pp. 4-24, 2020.

[6] C. Huang, T. Xu, and X. Wu, "Leader–Follower Formation Control of Magnetically Actuated Millirobots for Automatic Navigation," *IEEE/ASME Transactions on Mechatronics,* vol. 29, no. 2, pp. 1272-1282, 2024.

[7] X. Yan, D. Jiang, R. Miao *et al.*, "Formation Control and Obstacle Avoidance Algorithm of a Multi-USV System Based on Virtual Structure and Artificial Potential Field," *Journal of Marine Science and Engineering*, 2021.

[8] X. Chen, F. Huang, Z. Chen *et al.*, "A Novel Virtual-Structure Formation Control Design for Mobile Robots with Obstacle Avoidance," *Applied Sciences,* vol. 10, pp. 5807, 08/21, 2020.

[9] X. G. Guo, W. D. Xu, J. L. Wang *et al.*, "BLF-Based Neuroadaptive Fault-Tolerant Control for Nonlinear Vehicular Platoon With Time-Varying Fault Directions and Distance Restrictions," *IEEE Transactions on Intelligent Transportation Systems,* vol. 23, no. 8, pp. 12388-12398, 2022.

[10] Y. Li, Y. Zhao, W. Liu *et al.*, “Adaptive Fuzzy Predefined-Time Control for Third-Order Heterogeneous Vehicular Platoon Systems With Dead Zone,” *IEEE Transactions on Industrial Informatics,* vol. 19, no. 9, pp. 9525-9534, 2023.
[11] H. Zhang, J. Liu, Z. Wang *et al.*, “Distributed Adaptive Event-Triggered Control and Stability Analysis for Vehicular Platoon,” *IEEE Transactions on Intelligent Transportation Systems,* vol. 22, no. 3, pp. 1627-1638, 2021.
[12] J. Chen, H. Liang, J. Li *et al.*, “Connected Automated Vehicle Platoon Control With Input Saturation and Variable Time Headway Strategy,” *IEEE Transactions on Intelligent Transportation Systems,* vol. 22, no. 8, pp. 4929-4940, 2021.
[13] Y. Zheng, M. Xu, S. Wu *et al.*, “Development of Connected and Automated Vehicle Platoons With Combined Spacing Policy,” *IEEE Transactions on Intelligent Transportation Systems,* vol. 24, no. 1, pp. 596-614, 2023.
[14] Y. Li, Q. Lv, H. Zhu *et al.*, “Variable Time Headway Policy Based Platoon Control for Heterogeneous Connected Vehicles With External Disturbances,” *IEEE Transactions on Intelligent Transportation Systems,* vol. 23, no. 11, pp. 21190-21200, 2022.
[15] G. Guo, P. Li, and L. Y. Hao, “A New Quadratic Spacing Policy and Adaptive Fault-Tolerant Platooning With Actuator Saturation,” *IEEE Transactions on Intelligent Transportation Systems,* vol. 23, no. 2, pp. 1200-1212, 2022.
[16] S. Baldi, D. Liu, V. Jain *et al.*, “Establishing Platoons of Bidirectional Cooperative Vehicles With Engine Limits and Uncertain Dynamics,” *IEEE Transactions on Intelligent Transportation Systems,* vol. 22, no. 5, pp. 2679-2691, 2021.
[17] R. Liu, B. Qu, T. Wei *et al.*, "Research on UAV Formation Obstacle Avoidance Based on Consistency Control." pp. 155-160.
[18] J. Tang, B. Zhang, and S. Chai, "Lyapunov-based Model Predictive Control for the tracking of Nonholonomic Vehicle." pp. 587-592.
[19] Y. Díaz, J. Dávila, and M. Mera, “Leader-Follower Formation of Unicycle Mobile Robots Using Sliding Mode Control,” *IEEE Control Systems Letters,* vol. 7, pp. 883-888, 2023.
[20] J. Wang, X. Luo, L. Wang *et al.*, “Integral Sliding Mode Control Using a Disturbance Observer for Vehicle Platoons,” *IEEE Transactions on Industrial Electronics,* vol. 67, no. 8, pp. 6639-6648, 2020.
[21] J. Wang, X. Luo, J. Yan *et al.*, “Distributed Integrated Sliding Mode Control for Vehicle Platoons Based on Disturbance Observer and Multi Power Reaching Law,” *IEEE Transactions on Intelligent Transportation Systems,* vol. 23, no. 4, pp. 3366-3376, 2022.
[22] J. Boo, and D. Chwa, “Integral Sliding Mode Control-Based Robust Bidirectional Platoon Control of Vehicles With the Unknown Acceleration and Mismatched Disturbance,” *IEEE Transactions on Intelligent Transportation Systems,* vol. 24, no. 10, pp. 10881-10894, 2023.
[23] Q. Chen, L. Xu, Y. Zhou *et al.*, “Finite time observer-based super-twisting sliding mode control for vehicle platoons with guaranteed strong string stability,” *IET Intelligent Transport Systems,* vol. 16, no. 12, pp. 1726-1737, 2022.
[24] J. Zhou, D. Tian, Z. Sheng *et al.*, “Decentralized Robust Control for Vehicle Platooning Subject to Uncertain Disturbances via Super-Twisting Second-Order Sliding-Mode Observer Technique,” *IEEE Transactions on Vehicular Technology,* vol. 71, no. 7, pp. 7186-7201, 2022.
[25] C. K. Verginis, C. P. Bechlioulis, D. V. Dimarogonas *et al.*, “Robust Distributed Control Protocols for Large Vehicular Platoons With Prescribed Transient and Steady-State Performance,” *IEEE Transactions on Control Systems Technology,* vol. 26, no. 1, pp. 299-304, 2018.
[26] J. Wang, X. Luo, W. C. Wong *et al.*, “Specified-Time Vehicular Platoon Control With Flexible Safe Distance Constraint,” *IEEE Transactions on Vehicular Technology,* vol. 68, no. 11, pp. 10489-10503, 2019.
[27] J. Wang, W.-C. Wong, X. Luo *et al.*, “Connectivity-maintained and specified-time vehicle platoon control systems with disturbance observer,” *International Journal of Robust and Nonlinear Control,* vol. 31, no. 16, pp. 7844-7861, 2021.
[28] Y. Liu, D. Yao, H. Li *et al.*, “Distributed Cooperative Compound Tracking Control for a Platoon of Vehicles With Adaptive NN,” *IEEE Transactions on Cybernetics,* vol. 52, no. 7, pp. 7039-7048, 2022.
[29] Z. Gao, Y. Zhang, and G. Guo, “Fixed-Time Prescribed Performance Adaptive Fixed-Time Sliding Mode Control for Vehicular Platoons With Actuator Saturation,” *IEEE Transactions on Intelligent Transportation Systems,* vol. 23, no. 12, pp. 24176-24189, 2022.
[30] J. Zhao, X. Li, X. Yu *et al.*, “Finite-Time Cooperative Control for Bearing-Defined Leader-Following Formation of Multiple Double-Integrators,” *IEEE Transactions on Cybernetics,* vol. 52, no. 12, pp. 13363-13372, 2022.
[31] G. Guo, and Z. W. Zhao, “Finite-time terminal sliding mode control of connected vehicle platoons,” *Control Theory and Technology,* vol. 40, no. 1, pp. 149-159, 2023.